Focus on Fluids journals.cambridge.org/focus

Ultrasound rays in droplets: the role of viscosity and caustics in acoustic streaming

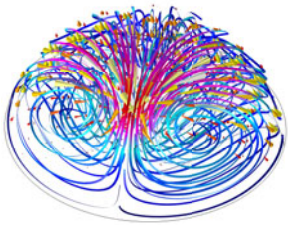

Henrik Bruus†

Department of Physics, Technical University of Denmark,
DTU Physics Building 309, DK-2800 Kongens Lyngby, Denmark

When an acoustic wave propagates through a viscous fluid, it progressively transfers momentum to the fluid through viscous dissipation, which results in the formation of a steady vortical flow called acoustic streaming. Although spawned by viscous effects, the magnitude of the streaming does not depend on the viscosity in most simple geometries. However, viscosity has a profound influence on the acoustic streaming as demonstrated by Riaud *et al.* (*J. Fluid Mech.*, vol. 821, 2017, pp. 384–420) in their study of sessile mm-sized water–glycerol droplets placed on a piezoelectric substrate with a 20-MHz ultrasound surface acoustic wave propagating along its surface. A detailed experimental and numerical analysis reveals that streaming dynamics is driven by a few ultrasound ray caustics inside the droplet.

Key words: acoustics, bubble dynamics, microfluidics

1. Introduction

The existence of steady streaming flow accompanying the propagation of acoustic waves in viscous fluids is a well known and ubiquitous phenomenon with a long history dating nearly 200 years back (Faraday 1831). Lord Rayleigh (1884) provided a theoretical explanation of this phenomenon, and his theory, extended by Schlichting (1932) to include acoustic boundary layers, describes one of the two basic mechanisms responsible for the force driving acoustic streaming: the shear stress that arises in the thin boundary layer near rigid walls, where the acoustic oscillatory bulk velocity of the fluid is forced to zero at the rigid walls by the no-slip boundary condition. Later, Eckart (1948) and Lighthill (1978) described the other mechanism responsible for streaming: the transfer of momentum by gradual absorption of the acoustic wave in the bulk of the fluid.

In the past two decades, interest in acoustic streaming has been revived by the application of ultrasound to manipulate fluids and suspended particles in microfluidic

† Email address for correspondence: bruus@fysik.dtu.dk

https://doi.org/10.1017/jfm.2017.420 Published online by Cambridge University Press

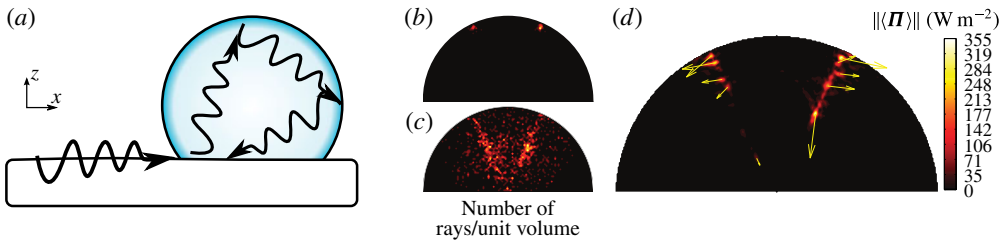

FIGURE 1. (*a*) Sketch of a 12-μL droplet placed on a piezoelectric lithium niobate substrate. A surface acoustic wave (SAW) propagates along the surface of the substrate and couples into the droplet, where it scatters at the droplet–air and droplet–solid interfaces. (*b*) Colour plot of the number of surface rays per unit volume from 0 (black) to 5×10^6 (white) revealing the surface caustic (white). (*c*) Same as (*b*) but for volume rays revealing the volume caustic (yellow through white). (*d*) Colour plot of the numerically calculated time-averaged Poynting vector $\boldsymbol{\Pi} = \langle \boldsymbol{v}p \rangle$ from 0 W m^{-2} (black) to 314 W m^{-2} (white). Adapted from Riaud *et al.* (2017).

systems (Wiklund, Green & Ohlin 2012). Especially two situations are of interest: the appearance of the streaming flow surrounding a suspended solid or fluid microparticle (Sadhal 2012*a*,*b*) and streaming generated inside a microfluidic channel (Muller *et al.* 2013; Lei, Glynne-Jones & Hill 2016). In spite of this revival of acoustic streaming, the effect of viscosity has long been ignored in acoustic streaming experiments.

2. Overview

The paper by Riaud *et al.* (2017) presents a detailed experimental and numerical study on the influence of viscosity and caustics on acoustic streaming in sessile 12-μL droplets containing a mixture of water and glycerol. As sketched in figure 1(*a*), the droplet, with a base diameter D between 3.7 and 4.0 mm, is resting on a piezoelectric lithium niobate substrate, along the surface of which a unidirectional monochromatic 20-MHz surface acoustic wave is propagating from left to right with the speed $c_{saw} =$ 3484 m s^{-1} and an amplitude of 62 pm. The acoustic wave is coupled into the droplet with great efficiency through the Rayleigh refraction angle θ_R, given by the Snell law $\sin\theta_R = c_0/c_{saw}$, where c_0 is the speed of sound in the droplet. This system is an excellent choice for the study at hand. By changing the glycerol mass fraction w_{gl} from 0 wt% to 90 wt% (in steps of 10 wt%), the dynamic viscosity η_0 increases by a factor of 175 from 0.89 to 156 mPa s while the bulk viscosity ξ increases by a factor of 64 from 2.8 to 182 mPa s. This leads to an increase by a factor of 40 in the ratio $\Lambda(w_{gl}) = D/L_a(w_{gl})$ between the droplet diameter D and the acoustic attenuation length L_a, and the experiments thus span from weak attenuation with $\Lambda(0\,\%) = 0.07$ in a pure water droplet to strong attenuation with $\Lambda(90\,\%) = 2.8$ in a 90 wt% glycerol droplet. All other droplet parameters vary much less with the glycerol content: the density ρ_0 between 1000 and 1230 kg m^{-3}, the speed of sound c_0 between 1510 and 1910 m s^{-1}, the acoustic wavelength λ_0 between 74 and 94 μm and the Rayleigh refraction angle between 26° and 33°.

The small acoustic wavelength relative to the droplet diameter, $\lambda_0/D \lesssim 0.02$, has three important implications. Firstly, the streaming is predominantly driven by bulk absorption and not by boundary layer stresses, secondly, the system may be analysed in terms of geometrical acoustics or ray acoustics, and thirdly, direct

https://doi.org/10.1017/jfm.2017.420 Published online by Cambridge University Press

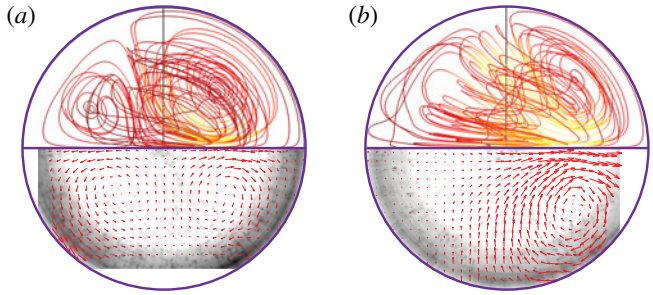

FIGURE 2. (*a*) Top view of streaming in a 12-μL 30 wt% glycerol droplet excited by a SAW propagating from left to right. The 4-vortex pattern is symmetric around the horizontal diameter. The coloured lines (upper half) are streamlines calculated numerically while the red arrows (lower half) represent measured streaming velocities with a maximum speed of 100 μm s^{-1}. (*b*) Same as (*a*) but showing a 2-vortex pattern in a 90 wt% glycerol droplet with a maximum speed of 10 μm s^{-1}. Adapted from Riaud *et al.* (2017).

numerical simulation based on standard methods may lead to prohibitive memory requirements. The latter technical problem is elegantly solved by the development of a new numerical scheme, called the streaming source spatial filtering method, which allows for grid cells larger than the small acoustic wavelength in the numerical simulations. Turning from numerics to physics, the ray analysis is illustrated in figure 1(*b*,*c*), where the number of surface and bulk rays per unit volume, respectively, are shown for the pure water droplet with low attenuation. The formation of a left–right symmetric V-shaped caustic is clearly seen, and its angle matches the Rayleigh refraction angle. Notably, this caustic coincides with the magnitude of the time-averaged Poynting vector as a function of position, shown in figure 1(*d*) and obtained by numerical simulation. The Poynting vector is the time-averaged product $\boldsymbol{\Pi} = \langle p\boldsymbol{v}\rangle$ of the acoustic pressure p and velocity $\boldsymbol{v}$, its spatial pattern is similar to that of the acoustic energy density and it gives the orientation of the flow forcing consistent with experiment. At low viscosity, the left–right symmetric caustics drives a left–right symmetric streaming pattern containing four vortices, as observed both experimentally and numerically, see figure 2(*a*). As the viscosity is increased by increasing the glycerol mass fraction, the acoustic rays attenuate before reaching the caustics at the back (left) and only the forward (right) branch of the caustic remains. This leads to the observed loss of left–right symmetry in the streaming pattern, as shown in figure 2(*b*), where only two vortices remain, both of them positioned in the forward (right) end of the droplet.

The results that the reader should take particular notice of can be summarized as follows: viscosity plays a crucial role in the dynamics and topology of acoustic streaming. The observed viscosity-driven topological transition has neither been reported nor explained so far in the literature. It is remarkable, how the carefully executed acoustic streaming experiments have been compared with good agreement to the numerical model developed from first principles, and including spatial filtering of the streaming source, which computes the acoustic streaming in three dimensions. Finally, it turns out that the force driving the acoustic streaming is mainly concentrated in a few caustics, whose position can be obtained easily from geometrical acoustics.

https://doi.org/10.1017/jfm.2017.420 Published online by Cambridge University Press

3. Future

The above study demonstrates convincingly how viscosity influences both the magnitude and the topology of acoustic streaming flow. This discovery marks an important progress in our understanding of acoustic streaming. So far, the analysis has only been carried out for sessile mm-sized droplets containing a homogeneous viscous fluid, but it will clearly play an important role in future studies of acoustic streaming in other and more complex systems. Examples of recently developed and more complex ultrasound-driven microfluidic systems, which would benefit of the new acoustic streaming analysis, are systems with rotating acoustic fields (Courtney *et al.* 2014; Riaud *et al.* 2014, 2015) and systems with inhomogeneous acoustic properties (Augustsson *et al.* 2016; Karlsen, Augustsson & Bruus 2016).

Currently, we are facing an exciting development in the nearly 200-year-old field of acoustic streaming, with respect to both our understanding of the underlying physics, and to applications of ultrasound in microfluidics. The work by Riaud *et al.* (2017) certainly stands out as an important contribution to this development.

References

AUGUSTSSON, P., KARLSEN, J. T., SU, H.-W., BRUUS, H. & VOLDMAN, J. 2016 Iso-acoustic focusing of cells for size-insensitive acousto-mechanical phenotyping. *Nat. Commun.* **7**, 11556.

COURTNEY, C. R. P., DEMORE, C. E. M., WU, H., GRINENKO, A., WILCOX, P. D., COCHRAN, S. & DRINKWATER, B. W. 2014 Independent trapping and manipulation of microparticles using dexterous acoustic tweezers. *Appl. Phys. Lett.* **104** (15), 154103.

ECKART, C. 1948 Vortices and streams caused by sound waves. *Phys. Rev.* **73**, 68–76.

FARADAY, M. 1831 On a peculiar class of acoustical figures; and on certain forms assumed by groups of particles upon vibrating elastic surfaces. *Phil. Trans. R. Soc. Lond.* A **121**, 299–340.

KARLSEN, J. T., AUGUSTSSON, P. & BRUUS, H. 2016 Acoustic force density acting on inhomogeneous fluids in acoustic fields. *Phys. Rev. Lett.* **117**, 114504.

LEI, J., GLYNNE-JONES, P. & HILL, M. 2016 Modal Rayleigh-like streaming in layered acoustofluidic devices. *Phys. Fluids* **28**, 012004.

LIGHTHILL, J. 1978 Acoustic streaming. *J. Sound Vib.* **61** (3), 391–418.

MULLER, P. B., ROSSI, M., MARIN, A. G., BARNKOB, R., AUGUSTSSON, P., LAURELL, T., KÄHLER, C. J. & BRUUS, H. 2013 Ultrasound-induced acoustophoretic motion of microparticles in three dimensions. *Phys. Rev.* E **88** (2), 023006.

RAYLEIGH, LORD 1884 On the circulation of air observed in Kundt's tubes, and on some allied acoustical problems. *Phil. Trans. R. Soc. Lond.* A **175**, 1–21.

RIAUD, A., BAUDOIN, M., BOU MATAR, O., THOMAS, J.-L. & BRUNET, P. 2017 On the influence of viscosity and caustics on acoustic streaming in sessile droplets: an experimental and anumerical study with a cost-effective method. *J. Fluid Mech.* **821**, 384–420.

RIAUD, A., BAUDOIN, M., THOMAS, J.-L. & BOU MATAR, O. 2014 Taming the degeneration of bessel beams at an anisotropic–isotropic interface: toward three-dimensional control of confined vortical waves. *Phys. Rev.* E **90**, 013008.

RIAUD, A., THOMAS, J.-L., BAUDOIN, M. & BOU MATAR, O. 2015 Taming the degeneration of bessel beams at an anisotropic–isotropic interface: toward three-dimensional control of confined vortical waves. *Phys. Rev.* E **92**, 063201.

SADHAL, S. 2012*a* Acoustofluidics 15: streaming with sound waves interacting with solid particles. *Lab on a Chip* **12**, 2600–2611.

SADHAL, S. S. 2012*b* Acoustofluidics 16: acoustics streaming near liquid–gas interfaces: drops and bubbles. *Lab on a Chip* **12** (16), 2771–2781.

SCHLICHTING, H. 1932 Berechnung ebener periodischer grenzeschichtströmungen. *Phys. Z.* **33**, 327–335.

WIKLUND, M., GREEN, R. & OHLIN, M. 2012 Acoustofluidics 14: applications of acoustic streaming in microfluidic devices. *Lab on a Chip* **12**, 2438–2451.

https://doi.org/10.1017/jfm.2017.420 Published online by Cambridge University Press